Methods for Partitioning the System and Performance Evaluation in Power-Hardware-in-the-Loop Simulations – Part II

Xin Wu
Ansoft Corporation
Four Station Square, Suite 200
Pittsburgh, PA, 15219
U.S.A
xwu@ansoft.com

Antonello Monti
Department of Electrical Engineering
University of South Carolina
300 Main St.,
Columbia, SC, 29208, USA
monti@engr.sc.edu

***Abstract* – In this paper, a novel method to determine the performance of the power-hardware-in-the-loop (PHIL) experiments is introduced. This method is based on wavelet transforms, and hence gives detailed information about the PHIL simulation results in terms of time and frequency. This method is used to compare the performance of the decoupled systems with different simulation/hardware interfaces introduced in Part I. Frequency analysis is also adopted to determine the performance of the PHIL experiments.**

I. INTRODUCTION

In Part I, different simulation/hardware interfaces for PHIL simulations are introduced, and their performances compared through the decoupled simulations of simple first-order systems. In [1], the authors analyzed the performance of the PHIL experiments based on system stability analysis. System stability analysis and visual inspection of the waveforms are not always sufficient in determining the performance of the PHIL experiments. The PHIL system can be stable while containing undesired transient, and/or yield results that are different from those of the original system. Therefore, it is necessary to find stricter criteria for performance analysis for PHIL experiments.

In this paper, a novel performance analysis method based on the wavelet theory is introduced. The ability to perform local analysis makes wavelet transform a better candidate than other signal processing methods for the analysis of signals that contain numerous non-stationary or transitory characteristics. Therefore, this performance analysis method gives the designer a better picture of the transients of the PHIL systems. This technique is demonstrated through the performance analysis of the PHIL experiments of the first-order systems with difference simulation/hardware interfaces, as described in Part I.

Furthermore, to determine how PHIL simulations match the behaviour of the actual system under different operation frequencies, frequency response analysis is performed on the original and the decoupled systems.

II. WAVELET ANALYSIS AND THE MALVAR WAVELETS

In general, when dealing with stationary signals whose statistical properties are invariant over time, the ideal tool for signal analysis is the Fourier transform. However, Fourier analysis has a serious drawback – when looking at the Fourier transform of a signal, it is impossible to tell when a particular event took place.

The short-time Fourier transform (STFT) represents a compromise between the time- and frequency-based views of a signal. The STFT provides some information about both when and at what frequencies a signal event occurs. The drawback of STFT is that once you choose a particular size for the time window, that window is the same for all frequencies. Many signals require a more flexible approach – one in which we can vary the window size to determine more accurately either time or frequency.

Wavelet analysis represents the next logical step: a windowing technique with variable-sized regions. Wavelet analysis allows the use of long time intervals where we want more precise low-frequency information, and shorter regions where we want high-frequency information [2].

In this research, this technique is adopted for the performance analysis of the PHIL experiments. The base functions of the Malvar wavelets used here are defined as:

$$\varphi_{j,k}(t) = \sqrt{\frac{2}{L_i}}\omega_j(t)\cos\left[\frac{\pi}{L_j}(k+\frac{1}{2})(t-a_j)\right] \quad (1)$$

Where $k=0,1,2,\ldots$, $j\in Z$, a_j is an increasing sequence of real numbers, L_j is the distance between a_j and a_{j+1}, $L_j=a_{j+1}-a_j$. The window function $\omega_j(t)$ is centred on the interval $[a_j,a_{j+1}]$. Assume that a sequence of positive numbers η_j is given such that $\eta_j+\eta_{j+1}\le L_j$ which ensures that the windows will only overlap with their nearest neighbour [3]. Here, $\omega_j(t)$ is defined as:

$$\omega_j(t) = \begin{cases} 1 & a_j+\eta_j \le t \le a_{j+1}-\eta_{j+1} \\ \sin\left[\frac{\pi}{2}\theta(\frac{t-a_j+\eta_j}{\eta_j})\right] & |t-a_j| \le \eta_j \\ \cos\left[\frac{\pi}{2}\theta(\frac{t-a_{j+1}+\eta_{j+1}}{\eta_{j+1}})\right] & |t-a_{j+1}| \le \eta_{j+1} \end{cases} \quad (2)$$

where $\theta(t) = \frac{1}{2}+\frac{15}{16}t-\frac{5}{8}t^3+\frac{3}{16}t^5$.

III. PERFORMANCE ANALYSIS BASED ON WAVELET TRANSFORMS

A. Performance Analysis for the First-Order System with the Inductive Load

In this section, the wavelet theory is utilized to study the transitory characteristics of the PHIL systems introduced in the Part I. Wavelet transform is applied to the error waveforms (*i.e.*, the difference between the waveforms from the decoupled simulation and those of the original system) using the Malvar wavelets.

Let us study the first-order system with the inductive load as introduced in Part I, whose parameters are listed in Table 1. It is noticed that the decoupled system with the Taganrog simulation/hardware interface has a long transient at the starting point, while the others have a relative smoother start-up. Apply wavelet transform to the beginning sections of the error waveforms and the results are shown in Fig. 1.

TABLE 1
PARAMETERS OF THE 1st-ORDER SYSTEM WITH THE INDUCTIVE LOAD

Component	Variable	Value
voltage source E (E(t)=Acos(2πft))	amplitude (A)	100V
	frequency (f)	50Hz
	resistance (R_1)	1Ω
load	resistance (R_2)	51Ω→1Ω
	inductance (L)	1mH

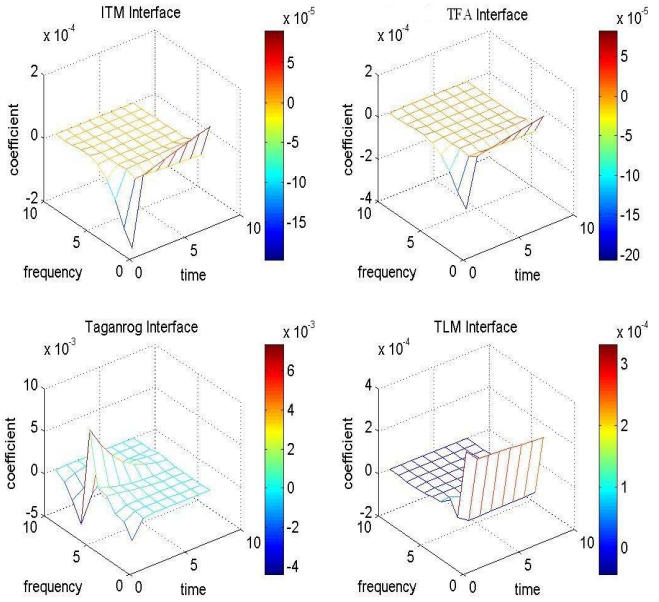

Fig. 1. The wavelet transform results of the error waveforms of I_{ROS}

The error waveforms under analysis have a time interval (0,1ms). The wavelet transform divides this time interval evenly into 8 time slices, and the frequency components of the signals into 10 frequency slices, with the highest frequency component being $f_{max}=1/2\times1/T_s=1/2\times1/1e\text{-}5=50kH_z$. In Fig. 1, the time axis corresponds to the time span of the signals, with 0 being equivalent to *t=0*, and 8 being equivalent to *t=1ms*. Similarly, the frequency axis corresponds to the frequency components of the signals, with the central frequency increasing as the number on the frequency axis increases. In other words, the higher number on the frequency axis represents the high frequency components of the signals, while lower ones stand for the low frequency components. The value of the central frequency of each frequency slice can be obtained through the Fourier transform of the corresponding wavelet. The coefficients obtained from the wavelets transform of the error waveforms provide time and frequency information about how the simulation results of the decoupled systems are different from the original results. If the coefficients are zero, it means that the decoupled system yields the same results as the original one; the higher the coefficients, the bigger the difference in the results.

Fig. 1 shows that the error waveform of the decoupled system with the Taganrog interface has some high frequency components at the beginning of the simulation, and the coefficients from wavelet transform are higher than the other error waveforms. This is consistent with the large oscillation shown in Fig. 20 of Part I. The error waveform of the decoupled system with the Ideal-Transformer-Model-(ITM-), the Time-Variant-First-Order-Approximation-(TFA-), and the Transmission-Line-Model-(TLM-)based interfaces have some low frequency components at the starting point, which correspond to the difference between the I_{ROS}_itm, I_{ROS}_tfa, I_{ROS}_tlm waveforms and that of the *I_org*.

Part I shows that the decoupled system with the TLM-based simulation/hardware interface has a long transient and large oscillation when the load changes at *t=50ms*. To obtain more information about the frequency response of this decoupled system to the dynamic change in the HUT, the wavelet transform is performed on the error waveform within the time interval (48ms, 53ms), and the results are shown in Fig. 2. The time interval is divided into 48 slices, and the frequency components into 10 slices. The arrow in the graph indicates the instant that the load changes. The high frequency components and their relatively large coefficients shown in Fig. 2 correspond to the big oscillation in the I_{ROS}_tlm waveform in Fig. 19 of Part I, while the low frequency components are consistent with the steady state error of I_{ROS}_tlm after the load changes shown in Fig. 19 of Part I.

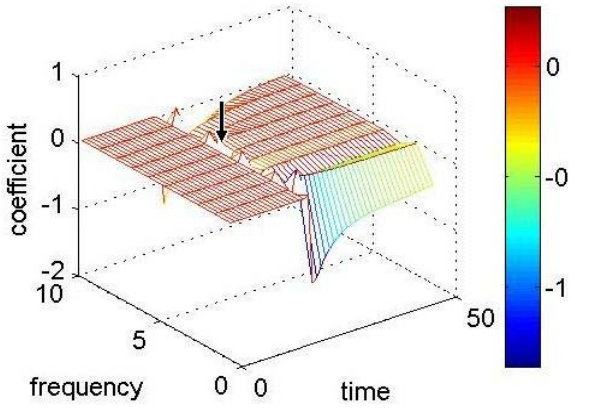

Fig. 2. The wavelet transform results of the error waveforms of I_{ROS} for the decoupled system with the TLM-based interface

B. Performance Analysis for the First-Order System with the Capacitive Load

The same analysis procedure in the previous section can be applied to the first-order system with the capacitive load as introduced in Part I, whose parameters are listed in Table 2. Similar to the previous case, when the load is inductive, the decoupled system with the Taganrog simulation/hardware interface has a long transient at the starting point, while the others have a relatively smoother start-up. Now let us apply wavelet transform to the beginning sections of the error waveforms; the results are shown in Fig. 3. The error

waveforms under analysis have a time interval (0, 1.8ms). The wavelet transform divides this time interval evenly into 16 time slices, and the frequency components of the signals into 10 frequency slices, with the highest frequency component being $f_{max}=1/2\times1/T_s=1/2\times1/1e\text{-}5=50kH_z$.

TABLE 2
PARAMETERS OF THE 1st-ORDER SYSTEM WITH THE CAPACITIVE LOAD

Component	Variable	Value
voltage source E (E(t)=Asin(2πft t))	amplitude (A)	100V
	frequency (f)	50Hz
	resistance (R_1)	51Ω
load	resistance (R_2)	51Ω → 1Ω
	capacitance (C)	1mF

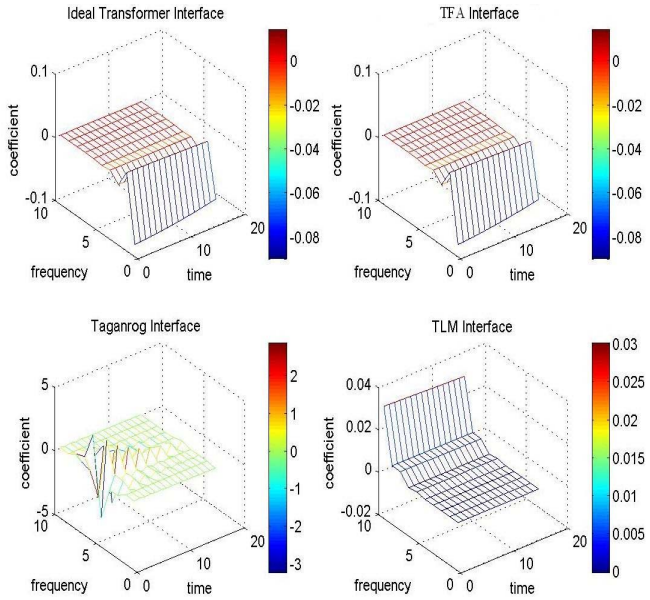

Fig. 3. The wavelet transform results of the error waveforms of V_{ROS}

Fig. 3 shows that the error waveform of the decoupled system with the Taganrog interface has some high frequency components at the beginning of the simulation, and the coefficients from the wavelet transform are one magnitude higher than the other error waveforms. The error waveforms of the decoupled system with the ITM-, the TFA- and the TLM-based interfaces have some low frequency components, which correspond to the steady state errors. Notice also that the error waveform of the decoupled system with the TLM-based interface has some constant high frequency components. This can be explained by zooming in on the V_{ROS} waveforms, as shown in Fig. 4. Therefore, the wavelet transform provides more detailed information about the decoupled simulation, which is not obvious from the relative error and the visual inspection of the waveforms.

From Fig. 24 in Part I, it seems that all the decoupled systems have a very smooth transition when the load changes at t=50ms. To obtain more information about the frequency response of this decoupled system to the dynamic change in the HUT, the wavelet transform is performed on the error waveforms within the time interval (48ms, 53ms); the results are shown in Fig. 5. The time interval is divided into 48 slices, and the frequency components into 10 slices. The arrow in the graphs indicates the instant that the load changes. Notice that the decoupled system with the ITM- and the TFA-based interfaces have a relatively smooth transition and the steady state errors decrease after the load change. There are some high frequency components in the error waveforms of the system with the Taganrog and the TLM-based interfaces, which correspond to the oscillation at the instant when the load changes. However, these are not obvious from the steady state errors or visual inspection of the waveforms.

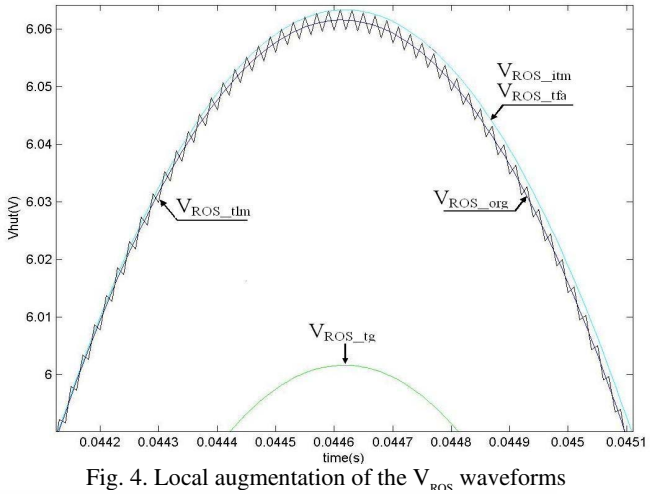

Fig. 4. Local augmentation of the V_{ROS} waveforms

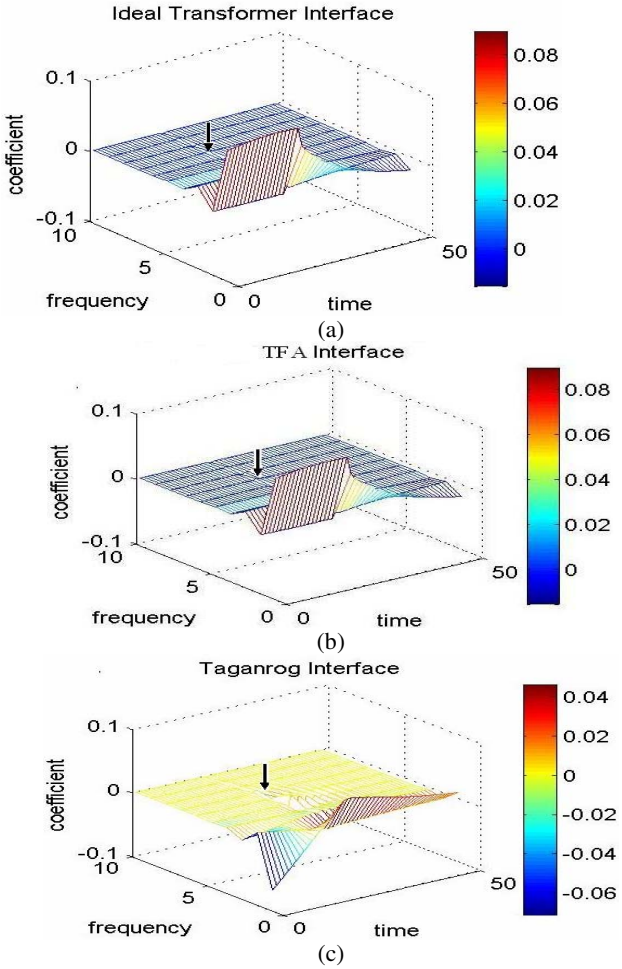

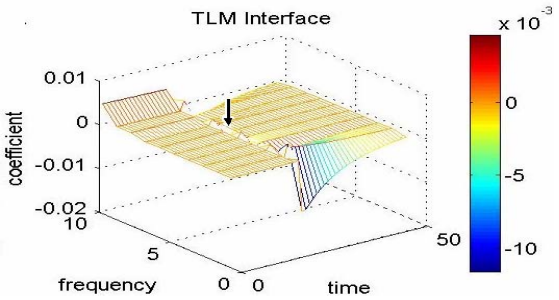

(d)

Fig. 5. The wavelet transform results of the error waveforms of V_{ROS}

IV. FREQUENCY RESPONSE ANALYSIS FOR PHIL EXPERIMENTS

The frequency response is a representation of the system's response to sinusoidal inputs at varying frequencies and is defined as the magnitude and phase differences between the input and output signals. Here, the system under study is a second-order system, and the Bode diagram is used to represent its frequency response. The original system is shown in Fig. 6, and its parameters listed in Table 3. This second-order system is implemented in the VTB, as shown in Fig. 7. The Frequency Analysis block provides a sinusoidal voltage source with amplitude of 10V, and a frequency that varies from 100Hz to 4KHz. The frequency response of the system is generated by comparing the current that goes into the circuit with the voltage reference, as shown in Fig. 8.

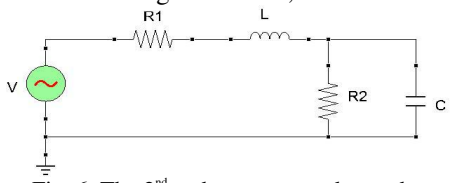

Fig. 6. The 2nd-order system under study

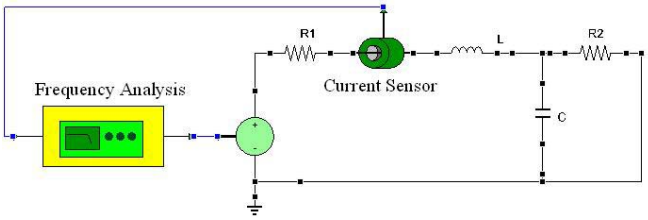

Fig. 7. VTB schematic for the frequency response analysis of the 2nd-order system

TABLE 3
PARAMETERS OF THE 2nd -ORDER SYSTEM UNDER STUDY – CONFIGURATION 1

Component	Variable	Value
voltage source V (V(t)=Asin(2πf t))	amplitude (A) frequency (f) resistance (R_1)	10V 100Hz~4KHz 1Ω
inductor L	inductance resistance	1mH 100 mΩ
capacitor C	capacitance resistance	1mF 100 mΩ
resistor R_2	resistance (R_2)	1Ω

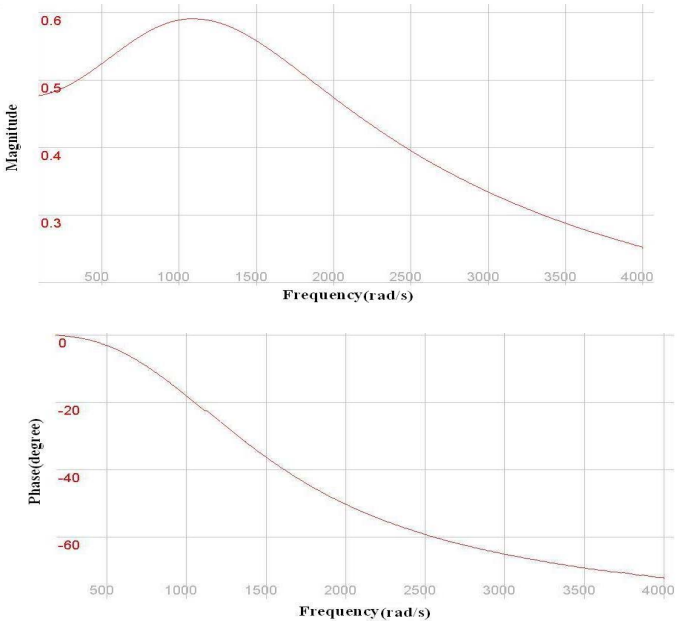

Fig. 8. Bode diagram of the original 2nd-order system (Configuration 1)

To determine how the PHIL simulation matches the behaviour of the actual system under different operation frequencies, frequency response analysis is performed on the original and the decoupled systems. With a simulation time step of 1μs, the frequency responses of the original system, the decoupled system with the ITM-based interface and the system with the interface based on TFA are shown in Fig. 9 (where ORG means the Bode diagram of the original system, and ITM and TFA mean that of the decoupled system with the ITM- and the TFA-based interface, respectively). The difference among the Bode diagrams of these three systems under this simulation time step is very small.

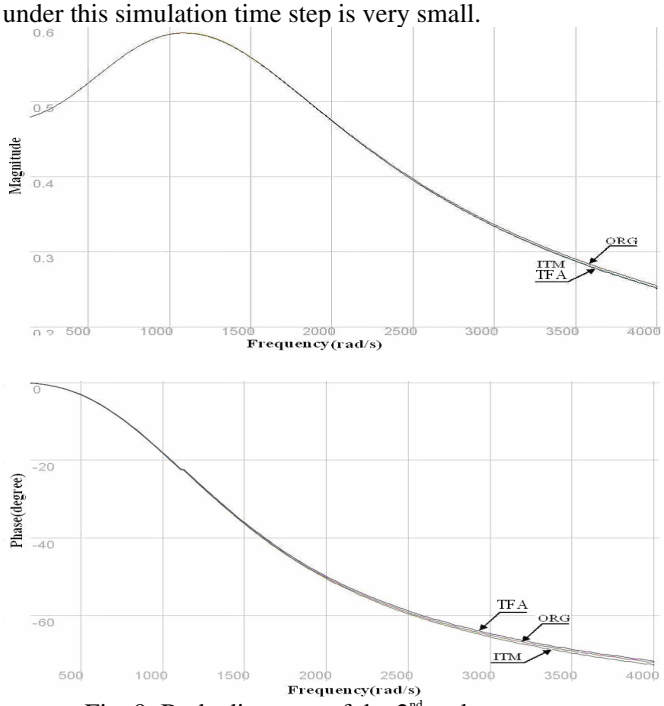

Fig. 9. Bode diagrams of the 2nd-order systems (configuration 2) from the VTB (Ts = 1μs)

Increasing the simulation time step to 10μs, the frequency responses of the original and the decoupled systems are shown in Fig. 10. There is a significant difference between the original system and the system with the ITM-based interface in the system gain at frequencies higher than 1KHz. This is because the delay effect in the ITM-based interface becomes increasingly significant as the simulation time step and the system operation frequency increase.

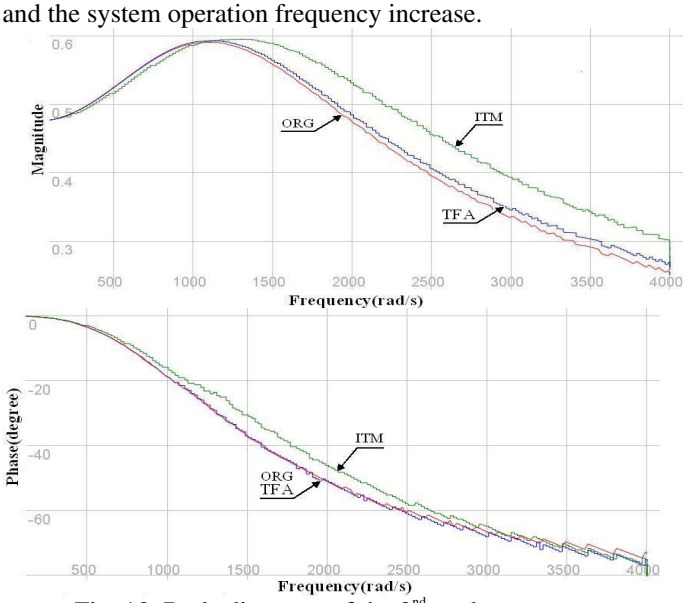

Fig. 10. Bode diagrams of the 2nd -order systems (configuration 1) from the VTB (Ts = 10μs)

Fig. 10 shows that the performance of the decoupled system varies with different system parameters, especially the decoupled system with the ITM-based interface. Both decoupled systems give a better approximation to the system in configuration 2 than that in configuration 1: the bode diagrams of the decoupled system are closer to that of the original system in the former case than the latter. In both cases, the decoupled system with the interface based on TFA gives better performance than the one with the ITM based interface, with closer approximation in the magnitude of the frequency response to the original system and smaller phase shift.

Next, let us change the parameters of the second-order system, as listed in Table 4. The frequency analysis is performed using a simulation time step of 10μs, and the frequency responses are shown in Fig. 11.

TABLE 4
PARAMETERS OF THE 2ind-ORDER SYSTEM UNDER STUDY – CONFIGURATION 2

Component	Variable	Value
Voltage source V (V(t)=Asin(2πf t))	amplitude (A)	10V
	frequency (f)	100Hz~4KHz
	resistance (R_1)	1Ω
inductor L	inductance	1mH
	resistance	100 mΩ
capacitor C	capacitance	10 mF
	resistance	100 mΩ
resistor R_2	resistance (R_2)	1Ω

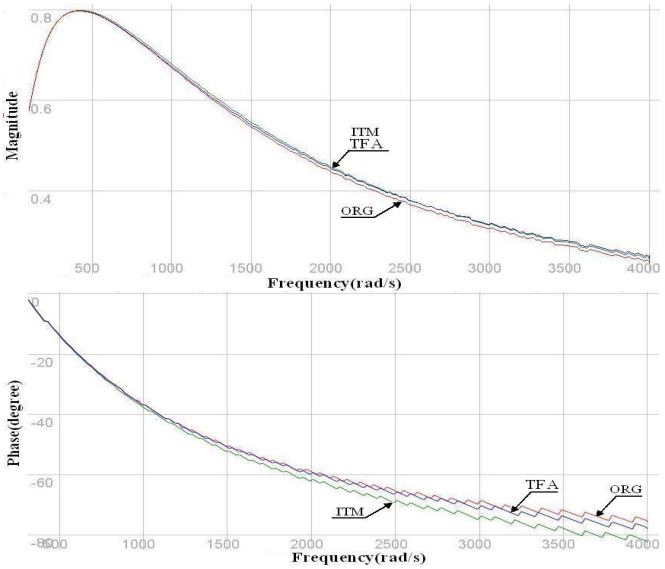

Fig. 11. Bode diagrams of the 2nd-order systems (configuration 2) from the VTB (Ts = 10μs)

The same frequency analysis procedure is applied to the same second-order system with another set of parameters, as listed in Table 5. The simulation time step is again chosen as10μs, and the frequency responses are shown in Fig. 12. In this case, the system gain of both decoupled systems is very close to that of the original system over the whole frequency range under analysis; while the decoupled system with the ITM-based interface has a bigger phase shift than the system with the TFA-based interface.

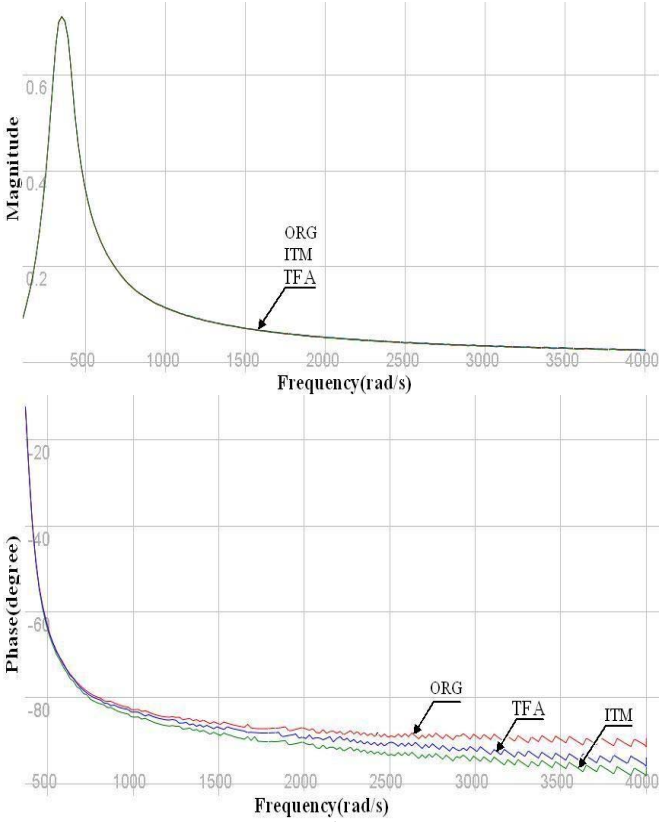

Fig. 12. Bode diagrams of the 2nd-order systems (configuration 3) from the VTB (Ts = 10μs)

TABLE 5
PARAMETERS OF THE 2nd-ORDER SYSTEM
UNDER STUDY – CONFIGURATION 3

Component	Variable	Value
voltage source V (V(t)=Asin(2πf t))	amplitude (A)	10V
	frequency (f)	100Hz~4KHz
	resistance (R_1)	1Ω
inductor L	inductance	10 mH
	resistance	100 mΩ
capacitor C	capacitance	1mF
	resistance	100 mΩ
resistor R_2	resistance (R_2)	51Ω

The above analysis concludes that the decoupled system with the simulation/hardware interface based on TFA has a frequency response that is closer to that of the original system than the system with the interface based on ITM. This can be further demonstrated through the comparison of the bandwidth of the decoupled PHIL systems. Here, the bandwidth of the PHIL system is defined as the frequency where the error in the magnitude or phase of the system frequency response is greater than the tolerable limit, *i.e.*, $BWPHIL=\{\omega | \Delta\angle H(j\omega)>\phi \text{ or } \Delta|H(j\omega)|>\xi\}$, where $\Delta\angle H(j\omega)$ and $\Delta|H(j\omega)|$ are the difference in the phase angle and the magnitude of the system frequency response between the original system and the decoupled system, respectively; ϕ and ξ are the tolerable limits of the phase angle and the magnitude errors. Choosing $\xi = 5$ degrees and $\xi = 3\%$, the bandwidth of the two decoupled second-order systems are compared under different system configurations, as shown in Table 6. Table 6 shows that when using the same simulation time step $Ts=10\mu s$, the decoupled system with the interface based on TFA has a bigger bandwidth than the system with the ITM-based interface. This means that while satisfying the performance requirements, the simulation/hardware interface based on TFA can be used in the PHIL experiments with a wider operation frequency range than the ITM-based interface.

TABLE 6
COMPARISON OF THE BANDWIDTH
OF THE DECOUPLED SYSTEMS

Configuration / System Bandwidth (Hz)	System configuration 1	System configuration 2	System configuration 3
decoupled system with the ITM-based interface	1190	1650	2930
decoupled system with the interface based on TFA	2890	2250	3030

V. CONCLUSIONS

In this paper, a novel performance analysis procedure based on the wavelet transform is proposed and adopted to determine the performance of the different simulation/hardware interfaces described in Part I. This novel performance analysis method provides the designer with the detailed and localized information about the dynamics of the PHIL experiments, which are hard to detect through relative errors and visual inspection of the signal waveforms.

The frequency response analysis is also adopted to determine the performance of the PHIL experiments. Both the wavelet transform method and the frequency response analysis demonstrate that the simulation/hardware interface based on TFA gives the best performance among all the interfacing schemes studied in this research.

VI. ACKNOWLEDGMENT

This work was supported in part by the U.S. Office of Naval Research under Grant N00014-02-1-0623 and N00014-03-1-0434.

V. REFERENCES

[l] S. Ayasun, A. Monti, R. Dougal, S. Vallieu, and R. Fischl. "On the Stability of Hardware in the Loop Simulation", *ELECTRIMACS 2002*, August 2002, Montreal, Canada.

[2] The MathWorks, Inc.. *Wavelet toolbox user's guide*, 2001.

[3] M. Vetterli, J. Kovacevic. *Wavelets and subband coding*. Prentice Hall PTR, NJ, 1995.

[4] S. Ayasun, S. Vallieu, R. Fischl, and T. Chmielewski. "Electric Machinery Diagnostic/Testing System and Power Hardware-In-the-Loop Studies", *Symposium on Diagnostics for Electric Machines, Power Electronics and Drives*. Aug. 2003, Atlanta, GA.

[5] S.Y.R. Hui and C. Christopoulos. "Numerical modeling of power circuits using transmission-line modeling". *Proc. IEEE on Power Electronics*. Vol. 6, No. 3, Oct. 1991, PP636-644.